

Accepted Manuscript

Design, synthesis and biological evaluation of new pyrazolyl-ureas and imidazopyrazolecarboxamides able to interfere with MAPK and PI3K upstream signaling involved in the angiogenesis

Elda Meta, Chiara Brullo, Adama Sidibe, Beat A. Imhof, Olga Bruno



PII: S0223-5234(17)30233-7

DOI: [10.1016/j.ejmech.2017.03.066](https://doi.org/10.1016/j.ejmech.2017.03.066)

Reference: EJMECH 9326

To appear in: *European Journal of Medicinal Chemistry*

Received Date: 19 December 2016

Revised Date: 9 March 2017

Accepted Date: 26 March 2017

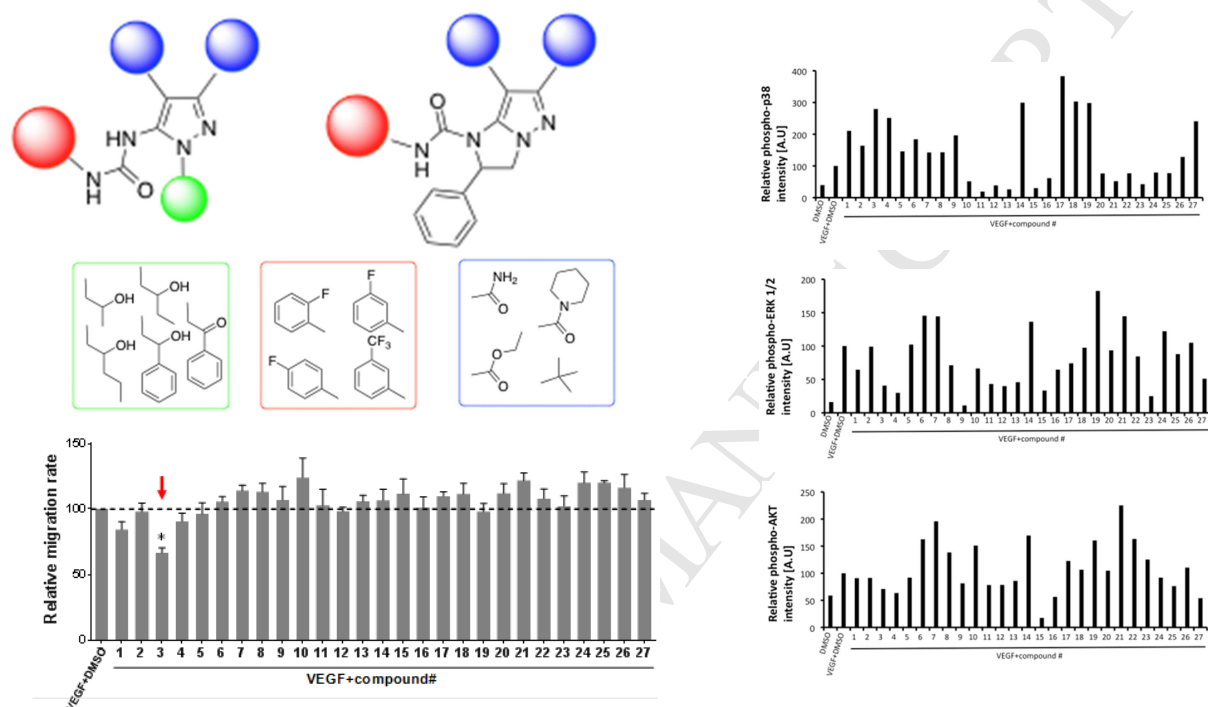
Please cite this article as: E. Meta, C. Brullo, A. Sidibe, B.A. Imhof, O. Bruno, Design, synthesis and biological evaluation of new pyrazolyl-ureas and imidazopyrazolecarboxamides able to interfere with MAPK and PI3K upstream signaling involved in the angiogenesis, *European Journal of Medicinal Chemistry* (2017), doi: 10.1016/j.ejmech.2017.03.066.

This is a PDF file of an unedited manuscript that has been accepted for publication. As a service to our customers we are providing this early version of the manuscript. The manuscript will undergo copyediting, typesetting, and review of the resulting proof before it is published in its final form. Please note that during the production process errors may be discovered which could affect the content, and all legal disclaimers that apply to the journal pertain.

Graphical abstract

Design, synthesis and biological evaluation of new pyrazolyl-ureas and imidazopyrazolecarboxamides able to interfere with MAPK and PI3K upstream signaling involved in the angiogenesis

Elda Meta, Chiara Brullo, Adama Sidibe, Beat A. Imhof and Olga Bruno



Design, synthesis and biological evaluation of new pyrazolyl-ureas and imidazopyrazolecarboxamides able to interfere with MAPK and PI3K upstream signaling involved in the angiogenesis

Elda Meta ^a, Chiara Brullo ^{a*}, Adama Sidibe ^b, Beat A. Imhof ^b and Olga Bruno ^a

^a *Department of Pharmacy, Medicinal Chemistry Section, University of Genoa, Viale Benedetto XV, 3 -16132 Genoa, Italy*

^b *Department of Pathology and Immunology, University of Geneva, Rue Michel-Servet 1-CH - 1211 Geneva, Switzerland*

Key words

p38MAPK phosphorylation; ERK1/2 phosphorylation; Akt phosphorylation; migration; pyrazolylureas; imidazopyrazole derivatives.

Abstract

Taking into account the structure activity relationship information given by our previous studies, we designed and synthesized a small library of pyrazolylureas and imidazopyrazolecarboxamides fluorinated on urea moiety and differently decorated on pyrazole nucleus. All compounds were preliminary screened by Western blotting technique to evaluate their activity on MAPK and PI3K pathways by monitoring ERK1/2, p38MAPK and Akt phosphorylation, and also screened with a wound healing assay to assess their capacity in inhibiting endothelial cell migration, using human umbilical vein endothelial cells stimulated with VEGF. Pyrazoles and imidazopyrazoles did not show the same activity profile. SAR consideration showed that specific substituents and their position in pyrazole nucleus, as well as the type of substituent on the phenylurea moiety play a pivotal role in determining increase or decrease of kinases phosphorylation. On the other hand the loss of flexibility in imidazopyrazole derivatives is responsible for activity potentiation. Screening of the compound library for inhibition of endothelial cell migration, a function required for angiogenesis, showed significant activity for compound **3**. This compound might interfere with cell migration by modulating the activity of different upstream target kinases. Therefore, compound **3** represents a potential inhibitor of angiogenesis. Furthermore, it may be used as a tool to identify unknown mediators of endothelial migration and thereby unveiling new therapeutic targets for controlling pathological angiogenesis in diseases such as cancers.

Abbreviations

Human umbilical vein endothelial cells, HUVECs; bone marrow-derived cells, BMDCs; basic fibroblast growth factor, bFGF; epithelial-mesenchymal transition, EMT; extracellular response kinases 1 and 2, ERK1/2; formyl-methyl-leucyl-phenylalanine peptide, fMLP; interleukine-8, IL-8, CXCL8; matrix metallo-proteinases 2, MMP-2; mitogen activated protein kinases, MAPKs; phosphatidylinositol 3-kinase, PI3K; protein kinases B, Akt/PKB; structure activity relationship, SAR; transforming growth factor- β , TGF- β ; vascular endothelial growth factor, VEGF.

1. Introduction

Angiogenesis consists in the formation of new blood vessels by sprouting from pre-existing ones; consequently it is vital for physiological processes during development and in the adult during wound healing, tissue growth and repair.

Pathological angiogenesis is required for the outcome of several diseases including cancers [1,2]. Indeed tumor cell hyperproliferation generates hypoxic areas inducing angiogenesis to rebuild oxygen and nutrient supply [3].

Physiological and pathological angiogenesis share similar mechanisms, one of them is the involvement of vascular endothelial growth factor (VEGF) and its receptors (VEGFR-1 and 2). Expression of VEGF is induced by hypoxia and is up-regulated in solid tumors [4, 5].

The VEGF/VEGFR axis induces key events such as endothelial cell sprouting, migration, proliferation and survival; VEGF induces these functions through activation of several serine/threonine kinases in the phosphatidylinositol 3-kinase (PI3K) signaling pathway including protein kinases B (Akt/PKB) and the mitogen-activated protein kinases (MAPK) signaling pathways such as extracellular response kinases 1 and 2 (ERK1/2) and p38MAPK. Finding new inhibitors that could affect the function of these kinases in endothelial cells would help to develop new potential therapeutic agents against pathological angiogenesis in solid cancers. Moreover, activation of ERK1/2 and p38MAPK was found crucial for other processes related to poor prognosis in cancers including epithelial to mesenchymal transition (EMT) (a typical process of the tumor cells), metastasis and recruitment of bone marrow-derived cells [6, 7]. This indicates that new drugs interfering with these mediator activities may target different components of the tumor microenvironment.

During our studies aimed at developing new anti-inflammatory drugs, we previously designed and synthesized different compound libraries able to inhibit the neutrophils chemotaxis by interfering with ERK1/2, Akt and p38MAPK phosphorylation after stimulation by Interleukine-8 (IL-8) or formyl-methyl-leucyl-phenylalanine peptide (fMLP) [8–13]. In particular, we demonstrated that our

pyrazolyl-urea (compounds **I**, Fig.1) differentially acted on ERK1/2, PI3K/Akt and p38MAPK phosphorylation depending on which chemoattractant (IL-8 or fMLP) was used [10]. A series of 4-carboxyethyl-pyrazole derivatives (compounds **II**, Fig. 1), bearing in N1 hydroxyalkyl chains characterized by different length, showed a notable increase of inhibitory activity, with respect to the previous compounds, inhibiting both fMLP-OMe- (a synthetic derivative of fMLP) and IL-8-induced chemotaxis at very low concentration (pM-nM range) [9]. We also reported the inhibitory effects of a little series of imidazo[1,2-*b*]pyrazole derivatives bearing in position 7 an acid, an ester or different amides substituents (compounds **III**, Fig. 1); implemented blocking effects was then evidenced by a library of more complex molecules containing the peculiar substituted urea moiety (typical of compounds **I** and **II**) fused with the more rigid structure of imidazopyrazole scaffold (compounds **IV**, Fig. 1) [11, 12]. All imidazopyrazoles inhibited fMLP-OMe or IL8-induced neutrophil chemotaxis in a dose-dependent manner with IC₅₀ values in the low nanomolar range. Further investigation evidenced that our inhibitors were able to significantly decrease PKC and p38MAPK phosphorylation after fMLP-OMe or IL-8 stimulation [13]. Notably, in the pyrazole series the 3-fluorophenylurea derivatives *in vivo* showed the most efficient chemotaxis inhibition [8,9].

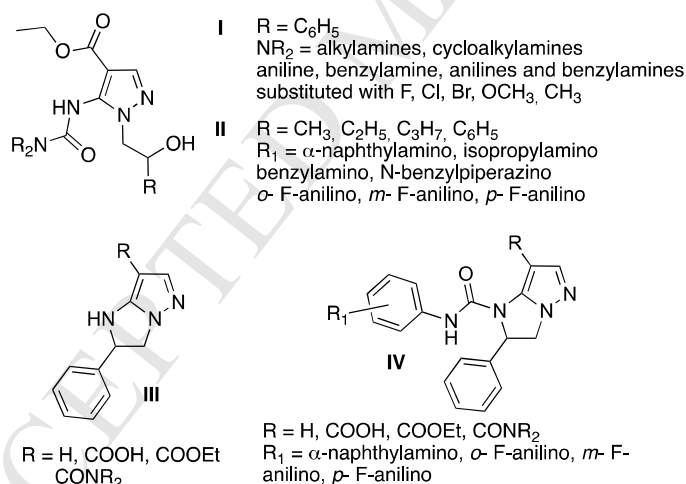


Fig. 1. General structure of compounds **I**, **II**, **III** and **IV**.

Given these potent inhibitory actions of our library compounds on MAPK activation and subsequent neutrophil chemotaxis, we aimed at designing and synthesizing new series of pyrazolylureas (compounds **1–16**, Fig. 2) and imidazopyrazolecarboxamides (compounds **17–27**, Fig. 2), that could interfere with MAPK and PI3K signaling pathways in endothelial cells during angiogenesis.

Taking into account the structure activity relationship (SAR) information given by previous studies, we functionalized the urea moiety in all new derivatives with a phenyl ring, bearing in turn

fluorinated substituents in different positions. Then, we combined old and new decorations, their type and position, both on the pyrazole and imidazopyrazole scaffold, to increase the molecular diversity.

In detail, the carboxyethyl substituent in position 4, which was typical for the previous compounds **I** and **II**, was maintained in **1–8**; the same hydroxyalkyl chains already present in compounds **II** were inserted in N1 (compounds **1–4**) while the hydroxyphenylethyl group was oxidized (compounds **5–8**) in order to modulate the lipophilicity of the molecules. As concerns the phenylurea moiety, we inserted in compound **1–4** a trifluoromethyl substituent in position 3, while compounds **5–8** were decorated with different fluorinated substituents in all positions. In compounds **9–16**, differently than in compounds **I** and **II**, a carboxyethyl or *t*-butyl substituent was inserted on position 3 of the pyrazole scaffold (position never investigated for our previous compounds). In addition we designed the new imidazopyrazoles **17–19** by maintaining in position 7 the most efficient substituents of previous **IV** (carboxyethyl, amide, piperidine-amide) while in the urea moiety we inserted the new 3-trifluoromethylphenyl substituent. Finally, compounds **20–27** were designed as more rigid analogues of compounds **9–16**.

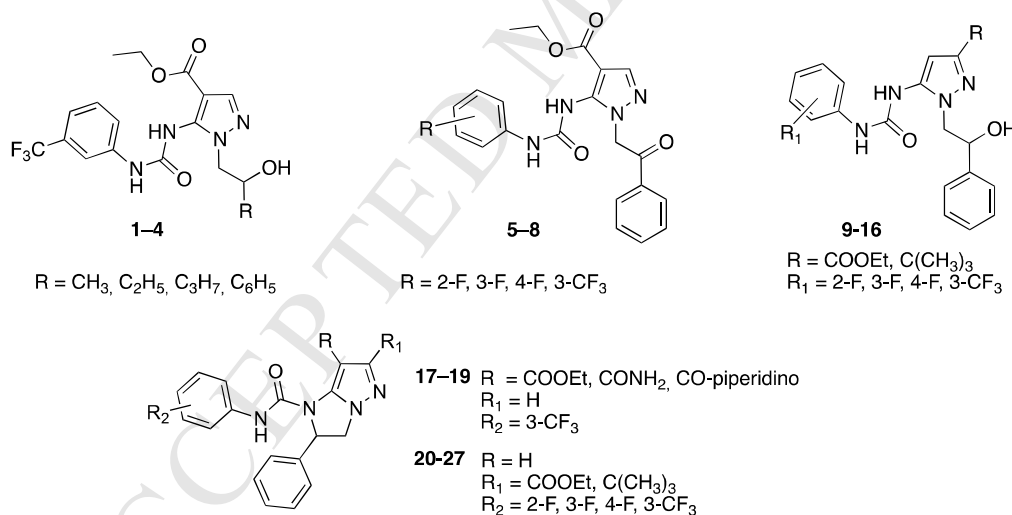


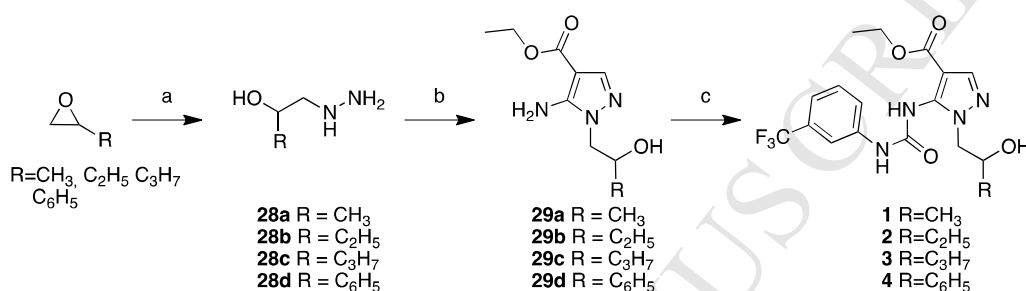
Fig. 2. General structures of compounds **1–27**.

All compounds were preliminary screened using Western blotting in order to evaluate their activity on the phosphorylation of ERK1/2, p38MAPK and Akt in human umbilical vein endothelial cells (HUVEC) stimulated with VEGF, and in a wound healing assay to evaluate the activity on endothelial cell migration upon VEGF stimulation. We report in this paper the synthesis, Western blot analyses and SAR considerations regarding the newly designed compounds **1–27**, as well as their activity on endothelial cell migration.

2. Results and discussion

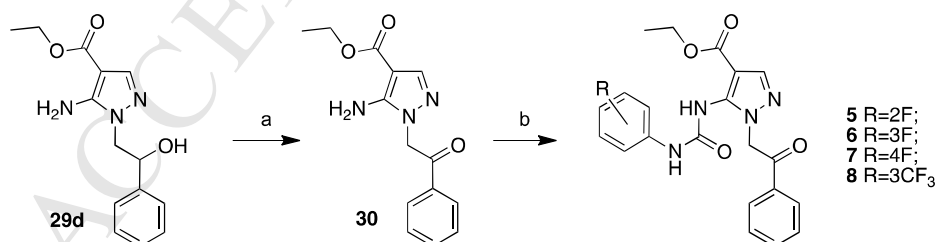
2.1 Chemistry

To obtain compounds **1–4** we condensed ethyl ethoxymethylenecyanoacetate with the hydrazino-hydroxyalkyl derivatives **28a–d**, which were in turn prepared by reaction of the appropriate oxirane with hydrate hydrazine, as previously reported [9]. The obtained intermediate 4-carboxyethyl-5-amino-pyrazoles **29a–d** were then treated with 3-trifluoromethylphenylisocyanate in anhydrous toluene affording the desired ethyl 3-(trifluoromethyl)phenylureido-pyrazole-4-carboxylates **1–4** (Scheme 1).



Scheme 1. Synthesis of compounds **1–4**. Reagents and conditions: (a) Hydrate hydrazine, 100 °C, 15 min, 70–82%; (b) Ethyl ethoxymethylenecyanoacetate, an. toluene, 70–80 °C, 8 h, 61–72%; (c) 3-trifluoromethyl-phenylisocyanate, an. toluene, reflux, 5h, 41–58%.

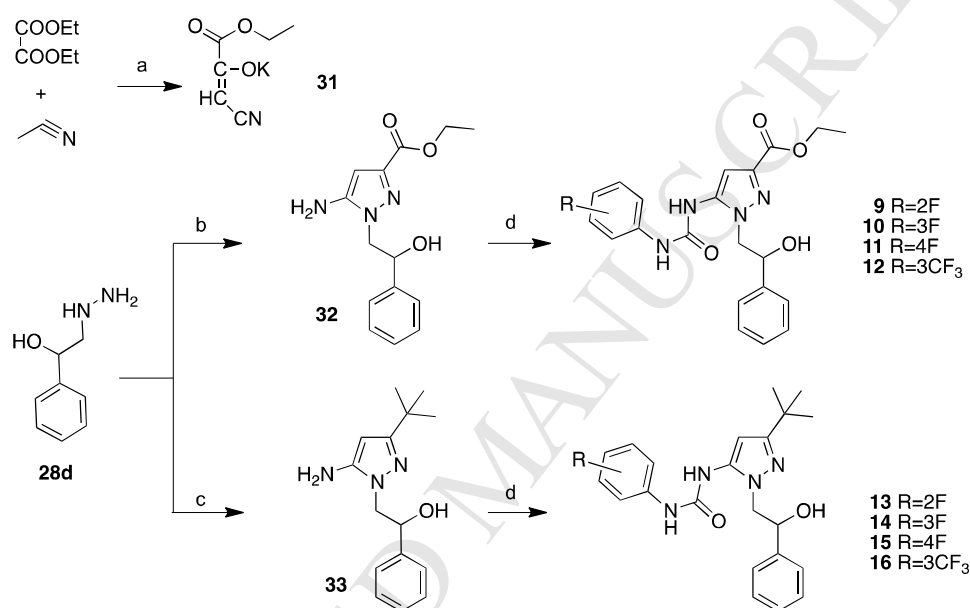
To prepare compounds **5–8** the hydroxy group of 4-carboxyethyl-5-amino-pyrazole **29d** was oxidized with sulphur trioxide pyridine complex in DMSO in the presence of triethylamine (TEA) affording the keton **30** (scheme 2), which was then reacted with a little excess of the suitable phenylisocyanate in anhydrous toluene at reflux giving the desired urea derivatives.



Scheme 2. Synthesis of compounds **5–8**. Reagents and conditions: (a) sulphur trioxide pyridine complex, DMSO, TEA, 20 °C, 30 min, 82%; (b) substituted phenylisocyanate, an. toluene, reflux, 12h, 32–55%.

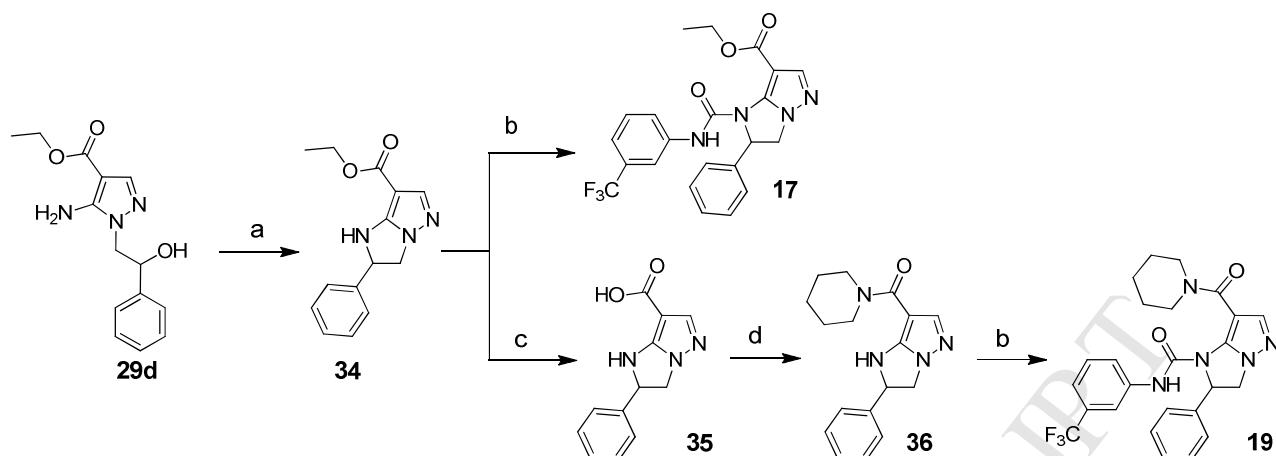
Compounds **9–12** and **13–16** were synthesized as reported in scheme 3. The key intermediate for the preparation of the pyrazole scaffold is the potassium salt of 1-cyano-3-ethoxy-3-oxoprop-1-en-2-olate **31** that was prepared following a literature procedure [14] by reacting acetonitrile with diethyloxalate in the presence of potassium *tert*-butoxide. The use of 18-Crown-6 as a catalyst

provided a strong increase in reaction yield in respect to the literature method. The obtained salt **31** was then condensed with the 2-hydrazino-1-phenylethanol **28d** in absolute ethanol in the presence of catalytic amount of glacial acetic acid yielding the ethyl 5-amino-1-(2-hydroxy-2-phenylethyl)-1*H*-pyrazole-3-carboxylate **32**. The same intermediate **28d** was reacted with the 4,4-dimethyl-3-oxopentanenitrile to obtain the 2-(5-amino-3-(*tert*-butyl)-1*H*-pyrazol-1-yl)-1-phenylethanol **33**. The reaction of **32** or **33** with a little excess of the suitable phenylisocyanate in anhydrous toluene at reflux gave the urea derivatives **9–12** and **13–16**, respectively.



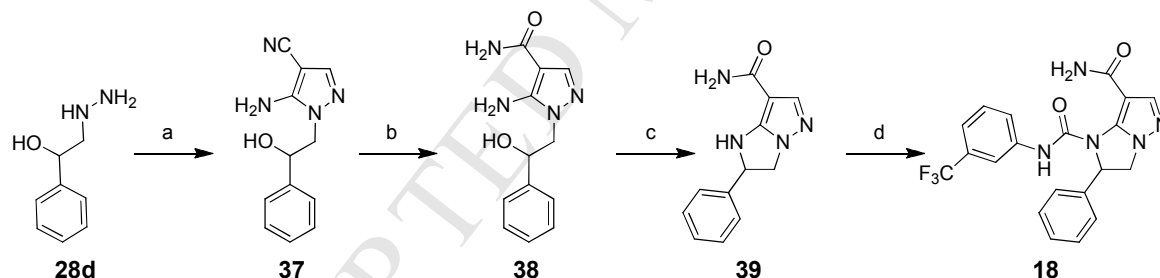
Scheme 3. Synthesis of compounds **9–16**. Reagents and conditions: (a) an THF, 18-Crown-6, 0–60 °C, 30 min, 98%; (b) **31**, abs. ethanol, conc. acetic acid, reflux 6 h, 59%; (c) 4,4-dimethyl-3-oxopentanenitrile, an. ethanol, conc. acetic acid, reflux, 10 h, 83%; (d) substituted phenylisocyanate, an. toluene, reflux, 6–12 h, 37–89%.

As previously reported [11], by dehydration of the 4-carboxyethyl-5-amino-pyrazole **29d**, we obtained the ethyl 2-phenyl-2,3-dihydro-1*H*-imidazo[1,2-*b*]pyrazole-7-carboxylate **34** (scheme 4). The carboxyethyl function of **34** was hydrolyzed to give carboxylic derivative **35** which was then reacted with an excess of piperidine in the presence of diphenylphosphorylazide (DPPA) to obtain the amide derivative **36**, as previously reported [11]. The treatment of **34** or **36** with a little excess of 3-trifluoromethyl-phenylisocyanate in anhydrous toluene at reflux afforded compounds **17** and **19**, respectively (Scheme 4).



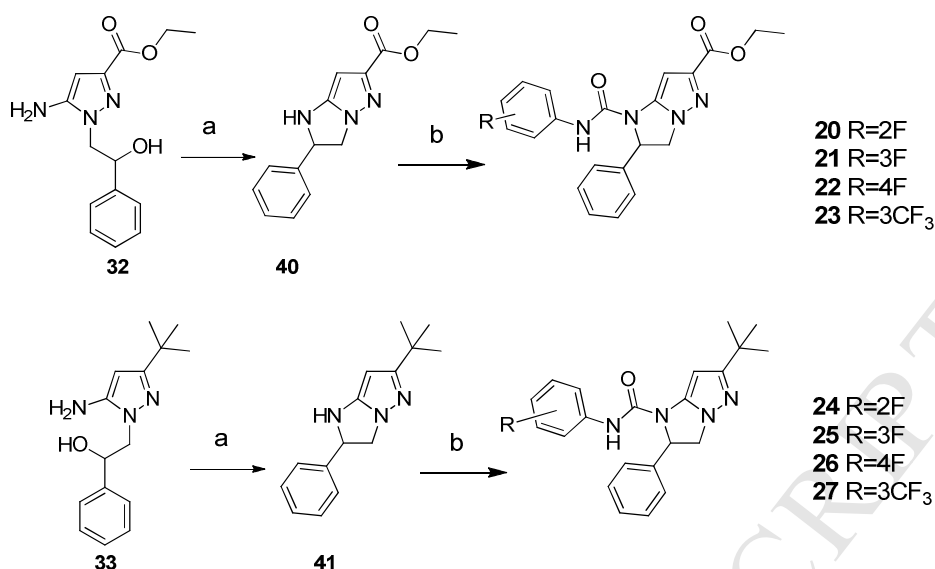
Scheme 4. Synthesis of compounds **17** and **19**. Reagents and conditions: (a) conc. H_2SO_4 , rt, 15 min, then NH_4OH , 80%; (b) 3-(trifluoromethyl)phenylisocyanate, an. DMF, reflux, 18 h, 36%; (c) 2M NaOH, EtOH, reflux, 4 h, 79%; (d) piperidine excess, an. DMF, DPPA, TEA, 30–60 °C, 12 h, 52%.

By condensation of 2-hydrazino-1-phenylethanol **28d** with ethoxymethylenemalononitrile we obtained the 5-amino-1-(2-hydroxy-2-phenylethyl)-1H-pyrazole-4-carbonitrile **37**, which was hydrolyzed to the amide derivative **38**; the latter was cyclized to the imidazopyrazole derivative **39** as previously reported [11], and finally we treated **39** with 3-trifluoromethylphenylisocyanate to give compound **18** (Scheme 5).



Scheme 5. Synthesis of compounds **18**. Reagents and conditions: (a) Ethoxymethylenemalononitrile, abs. EtOH, 70–80 °C, 6 h, 63%; (b) 2M NaOH, EtOH, reflux, 4 h, 65%; (c) conc. H_2SO_4 , rt, 15 min, then NH_4OH , 41%; (d) 3-(trifluoromethyl)phenylisocyanate, an. DMF, reflux, 18 h, 28%.

Starting from the above reported 3-substituted pyrazoles **32** and **33**, we obtained, by water elimination in the presence of concentrated sulfuric acid, the imidazopyrazoles **40** and **41**, respectively, which were treated with a little excess of the suitable substituted phenyl isocyanate in anhydrous toluene at reflux giving the imidazopyrazole-1-carboxamides **20–23** and **24–27**, respectively (Scheme 6).



Scheme 6. Synthesis of compounds **20–27**. Reagents and conditions: (a) conc. H₂SO₄, rt, 15 min., then NH₄OH, 78–80%; (b) substituted phenylisocyanate, an. toluene, reflux, 12–18 h, 27–83%.

2.2 Analysis of the compounds effects on MAPK and PI3K signaling pathways in HUVEC

The newly synthesized compounds were tested for their effects on the activation of MAPK and PI3K signaling pathways by monitoring p38MAPK, ERK1/2 and Akt phosphorylation induced by VEGF in HUVEC. Therefore, the compounds (**1–27**) were dissolved in DMSO and diluted in M199 medium to obtain a final solution at 20 μM concentration. Confluent HUVEC were starved for at least 4 h to reduce baseline kinase activities due to the serum in the culture medium. The cells were then incubated for 10 min with fresh medium containing the compounds or control DMSO and then stimulated with VEGF (50 ng/ml) and the indicated compound for 20 min. Then protein extracts were prepared and analyzed for phosphorylation of p38MAPK, ERK1/2 and Akt by Western blotting.

2.2.1 Compounds activities monitored with p38MAPK phosphorylation and SAR considerations

The activity of the compounds on p38MAPK phosphorylation is shown in Fig. 3. The most representative appearing bands and the relative densitometric analyses are shown. The results are expressed as percentage of control of the same blot (VEGF and DMSO only). Data are representative of at least two independent experiments. All new compounds (**1–27**) were able to interfere with the p38MAPK phosphorylation. Some of them decreased phosphorylation, others increased it. In particular, the 4-substituted pyrazoles (**1–8**) strongly increase phosphorylation, the most active being **3** (+ 180%) and **4** (+ 150%). The oxidation of the hydroxyalkyl chains (**5–8**) did not cause a relevant difference in phosphorylation increasing, therefore suggesting that neither the hydroxyl function nor the chiral center are important for the activity. Conversely the 3-substituted

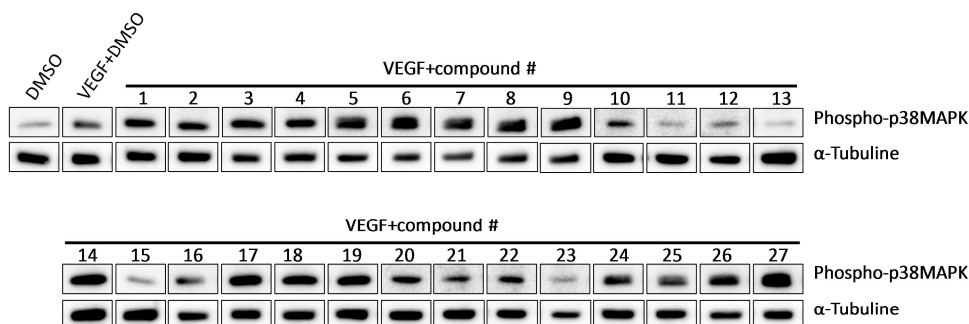
pyrazoles (**9–16**) generally showed a decrease, the most active being **11** (- 81%), **12** (- 61%), **13** (- 74%) and **15** (- 70%). Exceptions were observed for compounds **9** and **14** that strongly increased p38MAPK phosphorylation (+ 97% and + 199% respectively).

These results demonstrate that in VEGF-stimulated HUVEC, the 4-substitutions in pyrazole mainly interfered with the MAPK signaling pathways leading to increase of p38MAPK phosphorylation, whereas the 3-substitution in pyrazoles led to a blockade of p38MAPK phosphorylation as clearly evidenced by comparing the isomers **4** and **12**.

As concerns the more rigid imidazopyrazole derivatives (**17–27**) the Western blot revealed a behavior similar to that of pyrazole derivatives. In particular, all 7-substituted derivatives (**17–19**) strongly increased the p38MAPK phosphorylation (+ 200–300%), more than the flexible analogues 4-substituted pyrazoles. This indicates that in the 7-substituted imidazopyrazoles the structure rigidity may stabilize and improve the increasing effect, as it is clearly evidenced by comparing **17** with **4**.

The 6-substituted imidazopyrazoles (**20–26**), as their analogs 3-substituted pyrazoles, showed a moderate phosphorylation decrease. In this case the imidazopyrazole rigidity rendered them less potent toward decreasing p38MAPK phosphorylation. The only exception was compound **27** that showed a big increase (+ 140%).

A



B

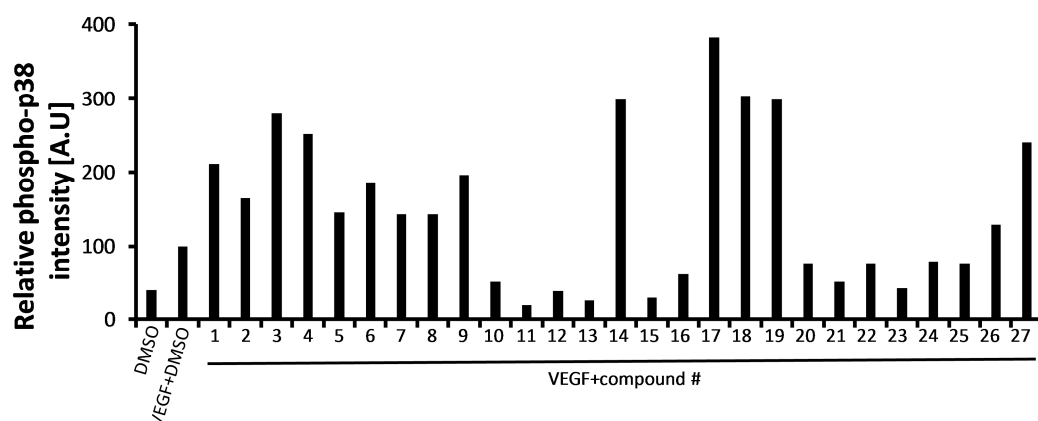


Fig. 3. Representative Western blotting analyses on p38MAPK phosphorylation. HUVEC were preincubated with the compounds for 10 min and then stimulated with both VEGF and the compounds for 20 min. DMSO was used as control. The proteins extracted and analyzed by western blotting, representative band of at least two independent experiments are reported (A). The densitometric analyses were done with ImageJ (B). Tubulin was used as the protein loading control. All compounds affected p38MAPK phosphorylation.

2.2.2 Compounds activities monitored with ERK1/2 phosphorylation and SAR considerations

The activity of the compounds (**1–27**) on the ERK 1/2 phosphorylation was measured in the same manner as for p38MAPK (Fig 4). Also in these experiments most of the compounds were able to interfere with the protein kinases phosphorylation. The pyrazole series **1–4** globally decreased ERK1/2 phosphorylation showing higher effect with longer chains at N1 of the pyrazoles. Exceptionally, compound **2** was inactive on ERK1/2 phosphorylation. Also the series **9–16** showed a general decrease of ERK1/2 phosphorylation. In these pyrazole series, compounds **3, 4, 9** and **15** showed the highest decrease (- 59%, - 70%, - 89%, - 67%, respectively).

The oxidation of the hydroxyalkyl chain did not cause a clear influence on this kinase activity, as two compounds (**6** and **7**) increased ERK1/2 phosphorylation, one (**8**) decreased it, while one (**5**) was inactive.

In the imidazopyrazole series, particularly in compounds **17–19**, the activity seems strictly to rely on the nature of the substituent in position 7. Indeed, compound **17**, bearing a 7-carboxyethyl group, showed slight decrease of ERK phosphorylation (- 26%), while the 7-piperidine amide **19** increased ERK phosphorylation (+ 83%). No activity was observed with the 7-amide derivative **18**. Of note, in general the 3-trifluoromethylphenylureas caused a stronger decrease of ERK phosphorylation, the most active being **23** (- 75%), with the only exception of **19** that strongly increased it.

SAR considerations on ERK and p38 phosphorylation are different showing that our derivatives may interfere at different upstream levels in the MAPK signaling pathways.

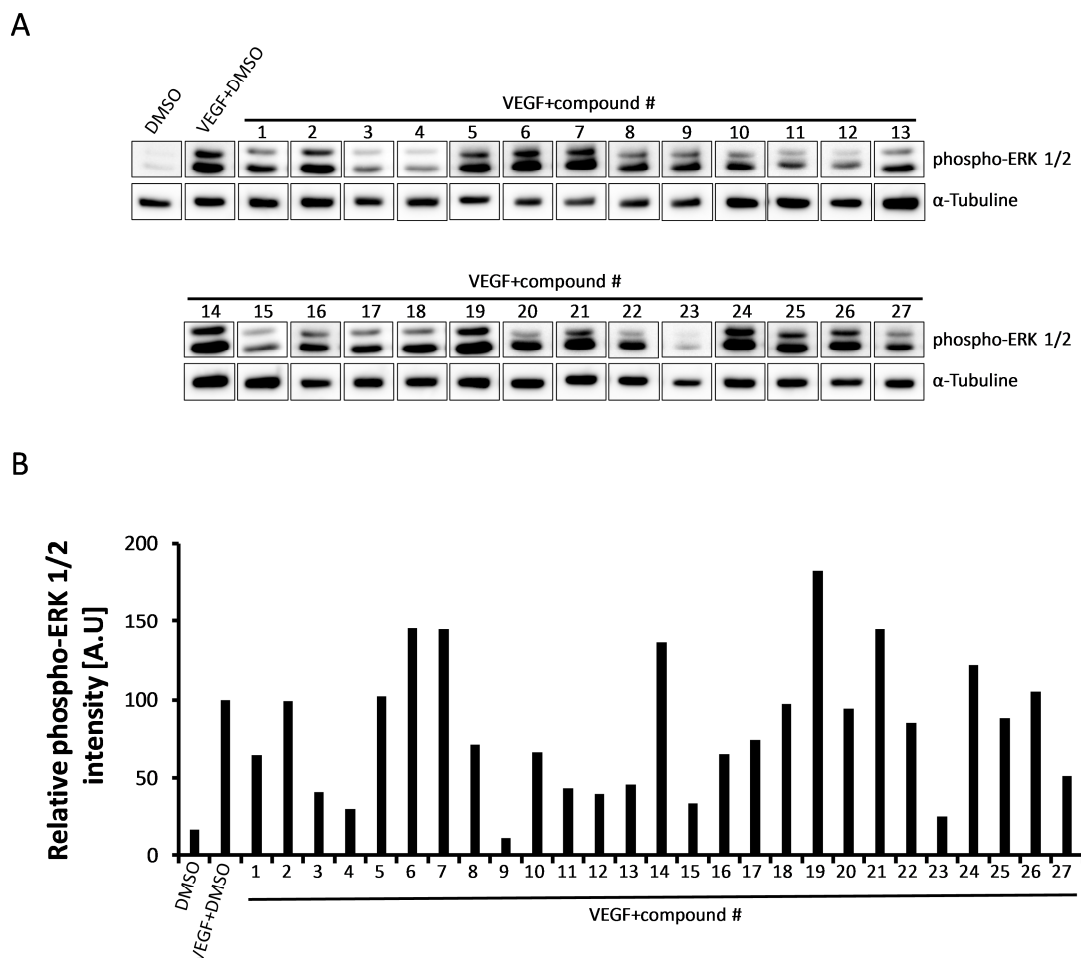


Fig. 4. Representative Western blotting analyses on ERK1/2 phosphorylation. HUVEC were preincubated with the compounds for 10 min and then stimulated with both VEGF and the compounds for 20 min. DMSO was used as control. The proteins extracted and analyzed by western blotting, representative band of at least two independent experiments are reported (A). The densitometric analyses were done with ImageJ (B). Tubulin was used as the protein loading control. Most of the compounds affected ERK1/2 phosphorylation.

2.2.3 Compounds activities monitored with Akt phosphorylation and SAR considerations

All compounds were also analyzed for their interference with PI3K signaling pathway in HUVEC upon VEGF stimulation. Therefore we analyzed their effect on Akt phosphorylation (Fig. 5). In the first pyrazole series (1–4) a moderate decrease of Akt phosphorylation was observed. Compounds **3** and **4** showed the highest effect (-29% and -37% respectively). This effect seemed to slightly correlate with the length of the chain in N1, as seen also for ERK1/2. The oxidation of the alcoholic group caused an inversion of the activity as clearly seen by comparing compound **4** (decrease) with its oxidized analogue **8** (increase). Interestingly, among this series (5–8) compounds **6** and **7**, bearing a 3-fluorophenyl and 4-fluorophenyl urea moiety respectively, showed the highest Akt phosphorylation increase (+ 63% and + 96%). It is to note that the 2-fluorophenyl urea derivative **5**,

as well as all the others 2-fluorophenyl urea derivatives in the other series (**9**, **13**, **20** and **24**), did not affect Akt phosphorylation.

The 3-carboxyethyl substituted pyrazoles **9–12** showed a poor decrease of Akt phosphorylation therefore indicating that the movement of the carboxyethyl group from position 4 (compounds **1–4**) to position 3 (compounds **9–12**) did not affect type of activity neither potency. Exception was the 3-fluorophenylurea derivative **10**, which showed strong increase (+ 51%). By introducing in position 3 a tert-butyl instead of a carboxyethyl group (series **13–16**), we obtained more potent inhibitors of Akt phosphorylation, being compound **15** the most active (- 83%). Interestingly, within this series compound **14**, which is a 3-fluorophenylurea derivative as **10**, is another exception. Indeed, **14** showed an increase of Akt phosphorylation, which was also stronger than that of the carboxyethyl derivative **10**. These results demonstrated that the 3-fluorophenylurea group determines an inversion of activity (from decrease to increase) towards Akt phosphorylation, while the tert-butyl substituent increments anyway the potency in respect with the carboxyethyl one.

In the imidazopyrazole series **17–23** we observed an increase of Akt phosphorylation. In particular by comparing the 3-carboxyethylpyrazole derivatives **9–12** with the analogue 6-carboxyethyl imidazopyrazoles **20–23**, we may suppose that the scaffold rigidity is responsible for the activity inversion (from decrease to increase) and for the implemented potency of the 3-fluorophenylurea derivative **21** in respect with **10**. Finally, the 6-tert-butyl derivatives **24–27** showed a different behavior in respect to the 6-carboxyethyl series **20–23** but there is not a clear structure activity relationship.

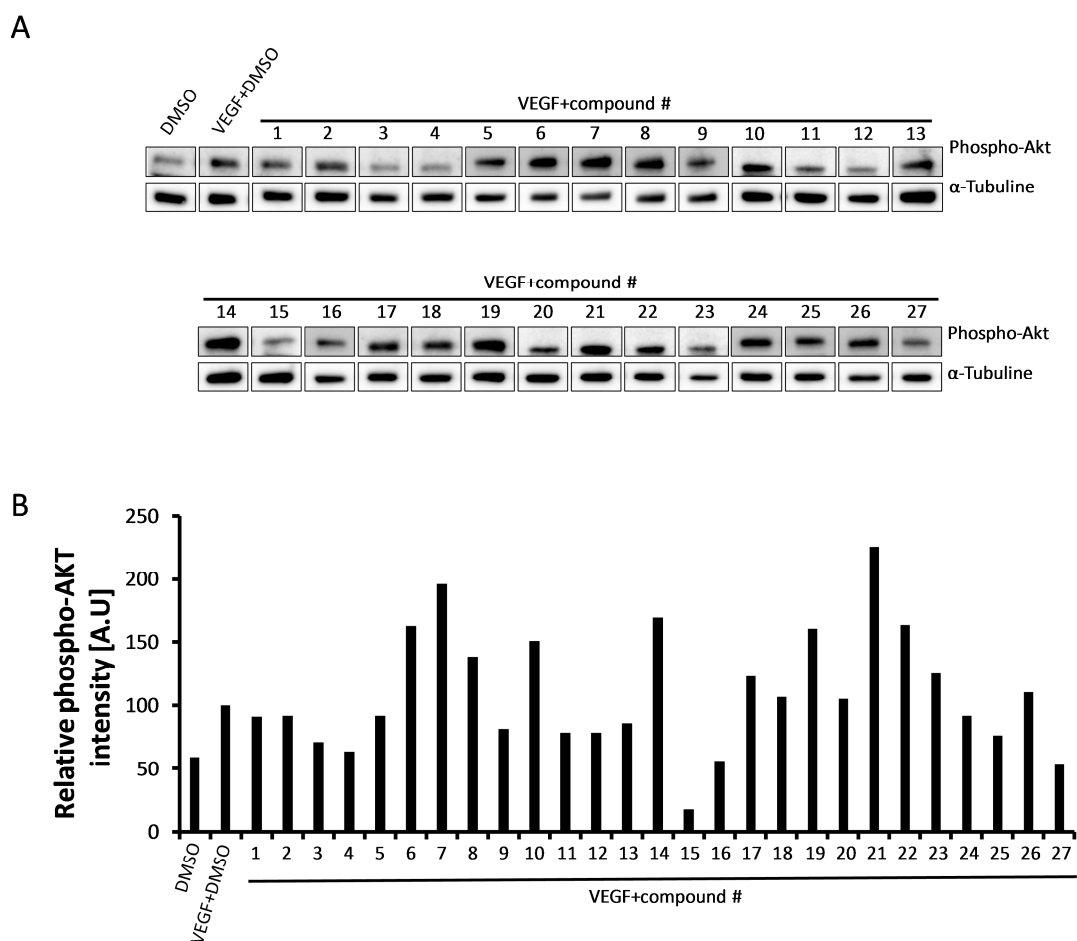


Fig. 5. Representative Western blotting analyses on Akt phosphorylation. HUVEC were preincubated with the indicated compound for 10 min and then stimulated with both VEGF and the compounds for 20 min. DMSO was used as control. The proteins extracted and analyzed by western blotting, representative band of at least two independent experiments are reported (A). The densitometric analyses were done with ImageJ (B). Tubulin was used as the protein loading control. Most of the compounds affected Akt phosphorylation.

2.3 Effect of compounds 1–27 on HUVEC migration in the wound healing assay.

As most of the compounds affected MAPK and PI3K signaling pathways likely through targeting different mediators, we tested their effect on endothelial cell (HUVEC) migration, a key function required for angiogenesis.

All compounds were screened using the wound healing assay upon VEGF stimulation.

Therefore, confluent HUVEC were injured with a sterile tip to create a scratch that they can heal by migrating toward the scratched area. The cells were washed with PBS and stimulated with VEGF in the presence of the indicated compound. The wounds were imaged just after VEGF addition and 15 h later with the ImageXpress microscope.

Only compound **3** showed a significant inhibitory effect on the HUVEC migration (Fig. 6, data are relative to the control set at 100 %). The compound **1** and **4** also showed trends toward inhibition of

endothelial cell migration, though not significant. Having the same pyrazole core and presenting similar modulatory profiles on p38MAPK, ERK1/2 and AKT phosphorylation, this inhibitory effect indicates that these molecular entities may be blockers of angiogenesis. Other compounds though strongly altered the phosphorylation of p38MAPK, ERK1/2 and AKT in endothelial cells stimulated by VEGF. For example, compound **15** that did not block endothelial cell migration and other derivatives even showed trends toward promotion of this cellular process. This suggests that the relationship between activation of these mediators of MAPK and PI3K signaling pathways in endothelial cells and subsequent migration of the cells is more complex than expected. This definitely demonstrated that the strict inhibition or activation of p38MAPK, ERK and AKT is not sufficient to block endothelial cell migration in contrast to other cells such as neutrophils. This also suggested that modulation of the activation patterns of other different mediators of MAPK and AKT may be a better strategy.

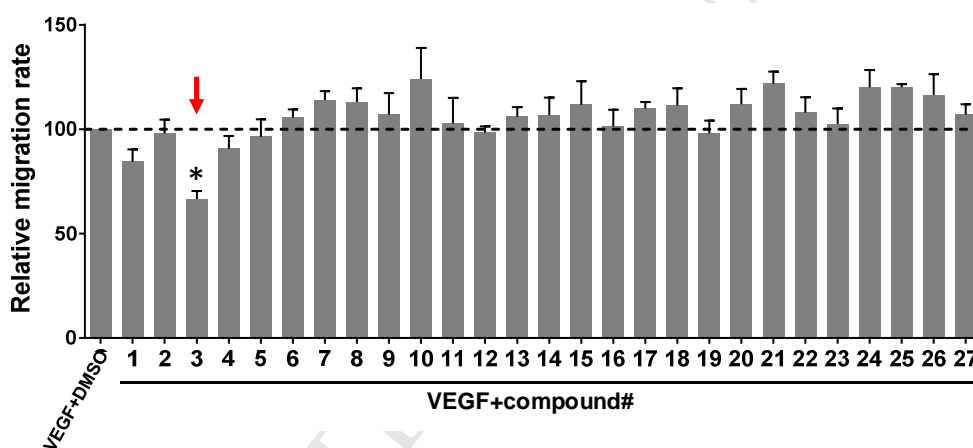


Figure 6. Representative migration analysis of compound **1–27** on wound healing assay. Confluent HUVEC were injured with a sterile tip to create a scratch and stimulated with both VEGF and the compounds, DMSO was used as control. The wounds were imaged just after VEGF addition and 15h later with the ImageXpress microscope. The area of the wound at time 0 and after 15 h was calculated with ImageJ. The reported data are relatively to the control set at 100%.

3. Conclusions

We report here design and synthesis of a new small library of pyrazole-ureas and imidazopyrazolecarboxamides, bearing a characteristic fluorophenyl substituent and different chemical substitution on pyrazole moiety never investigated in our previous studies.

To verify a possible action of these new derivatives on the MAPK and PI3K intracellular pathways we preliminarily screened them by monitoring ERK1/2, p38MAPK and Akt phosphorylation by Western blotting in human umbilical vein endothelial cells (HUVEC) stimulated with VEGF.

In general, all tested compounds showed a good ability in interfering with the phosphorylation of the studied kinases. However, the type of action (stimulation or inhibition of kinases phosphorylation) was different by considering each kinases on its own.

SAR considerations evidenced a pivotal role of the carboxyethyl position both in pyrazole and imidazopyrazole scaffold to interfere with the MAPK signaling pathways, leading to increase or decrease p38MAPK phosphorylation. In addition, in some imidazopyrazoles derivatives it is possible to observe an increase of potency clearly related to the flexibility loss in respect to the pyrazole analogues.

In the ERK1/2 both the pyrazoles and the imidazopyrazoles generally showed a decrease of phosphorylation, with few exceptions. A clear role in phosphorylation decrease was determined by length of chains at N1 on the pyrazoles **1–4**, while in the imidazopyrazole series **17–19** the activity seems strictly to rely on the nature of the substituent in position 7. Of note, in general the 3-trifluoromethylphenylureas caused a stronger decrease of ERK phosphorylation.

In Akt phosphorylation main pyrazoles showed a poor decrease of activity. Interestingly, results for compounds **10** and **14** demonstrated that the 3-fluorophenylurea group determines an inversion of activity (from decrease to increase) towards Akt phosphorylation, while the tert-butyl substituent increments anyway the potency in respect with the carboxyethyl one. Increasing activity on Akt phosphorylation, particularly evident in the 3-fluorophenylurea derivative **21**, was also determined by flexibility reduction in the imidazopyrazole derivatives.

In conclusion, the differently substituted forms of the pyrazoles and imidazopyrazoles did not show neither the same trends toward increasing or inhibiting p38MAPK, ERK1/2 and Akt phosphorylation, nor the same structure-activity relationship.

This may be explained partially by the crosstalk between different signaling pathways.

We could also speculate that the compound might interfere with different numbers of target kinases upstream of the monitored protein phosphorylation. However, altogether our results definitely showed that some structural features such as: 1) the type of substituent (carboxyethyl or ter-butyl) and their position (3 or 4) on the pyrazole; 2) the type of substitution on phenylurea moiety; 3) the flexibility loss in the imidazopyrazole derivatives in respect with pyrazoles ones, serve like a switch between increasing or decreasing the phosphorylation levels of p38MAPK, ERK1/2 and Akt and also determine the activity potency.

Despite their activities on the three kinases, most of the compounds did not inhibit endothelial cell migration; in fact the only one that showed a significant inhibition was compound **3**. Thus, in a next follow-up study it will be interesting to investigate its action on pathological angiogenesis and

identify the primary target kinases. This will be of fundamental importance also for identification of eventual unknown mediators of angiogenesis, thereby unveiling new therapeutic targets for controlling pathological angiogenesis in diseases such as cancer.

ACKNOWLEDGEMENTS

We thank Dr. M. Anzaldi, R. Raggio, Mr. O. Gagliardo, and F. Tuberoni for spectral recording and Mr. V. Ruocco for the informatics support to calculations.

This work has been supported by the University of Genoa (PRA 2013; PRA 2014), and grants from the Swiss National Science Foundation (310030-153456) and Oncosuisse (KFS-2914-02-2012) to BAI. The authors thank the Swiss Confederation for the Swiss Government Excellence Scholarship grant to EM.

CONFLICT OF INTEREST

The authors declare no conflict of interest.

AUTHORS INFORMATION

*Corresponding author: Chiara Brullo

Department of Pharmacy-Section of Medicinal Chemistry - School of Medical and Pharmaceutical Sciences – University of Genoa

Viale Benedetto XV, 3- 16132 Genoa, Italy

Phone: +39 010 353 8368

Fax: +39 010 353 8358

E-mail: chiara.brullo@unige.it

4. Experimental

4.1 Chemistry

Chiminord and Aldrich Chemical, Milan, Italy purchased all chemicals. Solvents were reagent grade. Unless otherwise stated, all commercial reagents were used without further purification.

Aluminium backed silica gel plates (Merck DC-Alufolien Kieselgel 60 F254, Darmstad, Germany), were used in thin-layer chromatography (TLC) for routine monitoring the course of reactions. Detection of spots was made by UV light. Merck silica gel, 230–400 mesh, was used for chromatography.

Melting points are not “corrected” and were measured with a Buchi M-560 instrument. IR spectra were recorded with a Perkin-Elmer 398 spectrophotometer. ^1H NMR spectra were recorded on a Varian Gemini 200 (200 MHz) instrument, chemical shifts are reported as δ (ppm) relative to

tetramethylsilane (TMS) as internal standard; signals were characterized as s (singlet), d (doublet), t (triplet), q (quartet), m (multiplet), br s (broad signal); J in Hz. Elemental analyses were determined with an elemental analyzer EA 1110 (Fison-Instruments, Milan, Italy) and the purity of all synthesized compounds was >95%.

4.1.1 General procedure for the synthesis of ethyl 1-(2-hydroxyalkyl)-5-(3-(3-(trifluoromethyl)phenyl)ureido)-1H-pyrazole-4-carboxylates **1–4**.

A mixture of the suitable 5-amino-1H-pyrazole-4-carboxylic acid ethyl esters (**29a–d**) (10 mmol) and 3-(trifluoromethyl)phenyl isocyanate (2 g, 11 mmol) in anhydrous toluene (70 mL) was refluxed for 6 h. After cooling to room temperature, the solution was washed with 3 M HCl (2 x 20 mL), with water (10 mL), dried (MgSO₄) and evaporated under reduced pressure. The crude crystallized by adding a solution of diethyl ether/petroleum ether (b.p. 50–60 °C) (1:1). The white solids obtained were recrystallized from absolute ethanol.

4.1.1.1 Ethyl 1-(2-hydroxypropyl)-5-(3-(3-(trifluoromethyl)phenyl)ureido)-1H-pyrazole-4-carboxylate **1**. White solid. Yield 41%; mp 160–161 °C. ¹H-NMR (DMSO-d₆): δ 1.24 (t, J = 7.0, 6H, 2CH₃), 3.30–3.42 (m, 2H, CH₂N), 4.08–4.22 (m, 3H, CH₂O e CHOH), 5.20 (br s, 1H, OH disappears with D₂O), 6.32 (m, 2H, 2NH, disappear with D₂O), 7.30–7.70 (m, 4H, Ar), 7.80 (s, 1H, H3). IR (KBr): cm⁻¹ 3430, 3340, 3265 (NH + OH), 1713 (COOEt), 1689 (CONH). Anal. (C₁₇H₁₉F₃N₄O₄) calcd for C, H, N.

4.1.2 Synthesis of ethyl 5-amino-1-(2-oxo-2-phenylethyl)-1H-pyrazole-4-carboxylate **30**.

A solution of sulphur trioxide pyridine complex (4.77 g, 30 mmol) in DMSO (20 mL) was added dropwise to a solution of ethyl 5-amino-1-(2-hydroxy-2-phenylethyl)-1H-pyrazole-4-carboxylate (**29d**) (2.75 g, 10 mmol) in DMSO (10 mL) and TEA (9 mL). The reaction mixture was stirred at 20–25 °C for 30 min. Then, 1M HCl solution was added until pH 5–6 and the reaction mixture was poured into water. The solid obtained was filtered and recrystallized from absolute ethanol. White solid. Yield: 82%; mp: 138–139 °C. ¹H-NMR (CDCl₃): δ 1.33 (t, J = 7.1, 3H, CH₃), 4.27 (q, J = 7.1, 2H, CH₂O), 5.10–5.20 (m, 2H, NH₂, disappears with D₂O), 5.48 (s, 2H, CH₂N), 7.45–7.75 (m, 4H, Ar), 8.02 (m, 1H, H3). IR (KBr): cm⁻¹ 3425, 3332 (NH₂), 1688 (CO), 1668 (COOEt). Anal. (C₁₄H₁₅N₃O₃) calcd for C, H, N.

4.1.3 General procedure for the synthesis of ethyl 1-(2-oxo-2-phenylethyl)-5-(3-phenylureido)-1H-pyrazole-4-carboxylates **5–8**.

A mixture of ethyl 5-amino-1-(2-oxo-2-phenylethyl)-1H-pyrazole-4-carboxylate (**30**) (2.73 g, 10 mmol) and the proper phenyl isocyanates (11 mmol) in anhydrous toluene (70 mL) was refluxed for 12 h. After cooling to room temperature, the solution was extracted with diethyl ether, washed with

3 M HCl (2 x 20 mL), with water (10 mL), dried (MgSO₄) and evaporated under reduced pressure. The crude crystallized by adding a solution of diethyl ether/petroleum ether (b.p. 50–60 °C) (1:1). The white solids obtained were recrystallized from absolute ethanol.

4.1.3.1 Ethyl 5-(3-(2-fluorophenyl)ureido)-1-(2-oxo-2-phenylethyl)-1H-pyrazole-4-carboxylate **5**.

White solid. Yield 32%; mp: 159–161 °C. ¹H-NMR (CDCl₃): δ 1.43 (t, *J* = 7.0, 3H, CH₃), 4.30 (q, *J* = 7.0, 2H, CH₂O), 5.90 (s, 2H, CH₂N), 6.90–8.40 (m, 12H, 9Ar + H₃ + 2NH, 2H disappear with D₂O). IR (CHCl₃): cm⁻¹ 3020 (NH), 1720–1650 (COOEt + CONH + CO). Anal. (C₂₁H₁₉FN₄O₄) calcd for C, H, N.

4.1.4 Synthesis of potassium 1-cyano-3-ethoxy-3-oxoprop-1-en-2-olate **31**.

Diethyl oxalate (0.44 g, 2.9 mmol) was slowly added at 0 °C to a solution of potassium *t*-butoxide (0.34 g, 3 mmol) in an. THF (27 mL) in the presence of 18-Crown-6 (0.63 g, 2.4 mmol). The mixture was heated until 60 °C, acetonitrile (0.12 g, 3 mmol) was slowly added and the mixture was heated at 60 °C for 30 min. After cooling to room temperature a yellow solid was obtained, which was collected by filtration and used in the following step as crude. Yield: 98%. (let. 78% [14]).

4.1.5 Synthesis of ethyl 5-amino-1-(2-hydroxy-2-phenylethyl)-1H-pyrazole-3-carboxylate **32**.

A mixture of 2-hydrazino-1-phenylethanol (**28d**) (1.52 g, 10 mmol), potassium 1-cyano-3-ethoxy-3-oxoprop-1-en-2-olate (1.79 g, 10 mmol) and glacial acetic acid (1 mL) in absolute ethanol (10 mL) was heated at reflux for 6 h. After cooling to room temperature, the solvent was evaporated, and the residue was dissolved in water and extracted with ethyl acetate (3 x 20 mL). The combined organic phases were then washed with NaHCO₃ sat. solution (20 mL), brine (20 mL) and twice with water (2 x 20 mL), dried (MgSO₄) and evaporated under reduced pressure. The crude was then purified by Silicagel column chromatography using diethyl ether as the eluent. White solid. Yield 59%, mp 121–122 °C. ¹H-NMR (CDCl₃): δ 1.37 (t, *J* = 7.0, 3H, CH₃), 3.48 (br s, 3H, NH₂ + OH, 1H disappears with D₂O), 4.10–4.43 (m, 4H, CH₂N + CH₂O), 5.07–5.20 (m, 1H, CHOH), 6.03 (s, 1H, H₄), 7.24–7.45 (m, 5H, Ar). IR (KBr): cm⁻¹ 3484 (OH), 3386, 3306 (NH₂), 1727 (CO). Anal. (C₁₄H₁₇N₃O₃) calcd. for C, H, N.

4.1.6 General procedure for the synthesis of ethyl 1-(2-hydroxy-2-phenylethyl)-5-(3-phenylureido)-1H-pyrazole-3-carboxylates **9–12**.

A mixture of ethyl 5-amino-1-(2-hydroxy-2-phenylethyl)-1H-pyrazole-3-carboxylate (**32**) (2.7 g, 10 mmol) and the suitable phenyl isocyanate (11 mmol) in anhydrous toluene (30 mL) was refluxed for 6 h. After cooling to room temperature, the white solid obtained was filtered and recrystallized from absolute ethanol.

4.1.6.1 Ethyl 5-(3-(2-fluorophenyl)ureido)-1-(2-hydroxy-2-phenylethyl)-1H-pyrazole-3-carboxylate 9. White solid. Yield 65%; mp 91–92 °C. ¹H-NMR (CDCl₃): δ 1.21 (t, *J* = 7.0, 3H, CH₃), 3.20 (br s, 1H, OH, disappears with D₂O), 4.05–4.60 (m, 4H, CH₂N + CH₂O), 4.95–5.10 (m, 1H, CHOH), 6.78–7.32 (m, 9H, Ar), 7.63–8.70 (m, 3H, H₄ + 2NH, 2H disappear with D₂O). IR (CHCl₃): cm⁻¹ 3420–3050 (OH + NH), 1735–1690 (COOEt + CONH). Anal. (C₂₁H₂₁FN₄O₄) calcd for C, H, N.

4.1.7 Synthesis of 2-(5-amino-3-tert-butyl-1H-pyrazol-1-yl)-1-phenylethanol 33.

4,4-dimethyl-3-oxopentanenitrile (1.25 g, 10 mmol) and concentrated acetic acid (0.20 mL) were added to a solution of 2-hydrazino-1-phenylethanol (**28d**) (1.52 g, 10 mmol) in absolute ethanol (20 mL) and the reaction mixture was refluxed for 10 h. The solvent was evaporated under reduced pressure and a crude solid crystallized by adding a solution of diethyl ether/petroleum ether (b.p. 50–60°C) 1/1. Yellow solid. Yield: 83%; mp: 131–133 °C. ¹H-NMR (DMSO-d₆): δ 1.20 (s, 9H, 3CH₃), 3.80–4.00 (m, 2H, CH₂N), 4.80–5.00 (3H, CHOH + NH₂, 2H disappear with D₂O), 5.20 (s, 1H, H₄), 5.85 (br s, 1H, OH, disappears with D₂O), 7.20–7.40 (m, 5H, Ar). IR (CHCl₃): cm⁻¹ 3500–3000 (NH₂ + OH). Anal. (C₁₅H₂₁N₃O) calcd for C, H, N.

4.1.8 General procedure for the synthesis of 1-(3-(tert-butyl)-1-(2-hydroxy-2-phenylethyl)-1H-pyrazol-5-yl)-3-phenylureas 13–16.

A mixture of 2-(5-amino-3-tert-butyl-1H-pyrazol-1-yl)-1-phenylethanol (**33**) (2.59 g, 10 mmol) and the suitable phenyl isocyanate (11 mmol) in anhydrous toluene (100 mL) was refluxed for 12 h. The solvent was evaporated under reduced pressure and the crude was dissolved in DCM (50 mL), washed with 3M HCl (2 x 20 mL), water (10 mL), dried (MgSO₄) and evaporated under reduced pressure. The solid obtained was crystallized from DCM, or, if necessary, purified by chromatography on Silica gel using a mixture of DCM/CH₃OH (8:2) as eluent.

4.1.8.1 1-(3-(tert-butyl)-1-(2-hydroxy-2-phenylethyl)-1H-pyrazol-5-yl)-3-(2-fluorophenyl)urea 13.

White solid. Yield: 37%; mp: 96–99 °C. ¹H-NMR (CDCl₃): δ 1.26 (s, 9H, 3CH₃), 4.08–4.39 (m, 2H, CH₂N), 5.03–5.19 (m, 1H, CHOH), 6.17 (s, 1H, H₄), 6.90–7.60 and 8.03–8.20 (2m, 11H, 9Ar + 2NH, 2H disappear with D₂O). IR (CHCl₃): cm⁻¹ 3400–3000 (NH + OH), 1708 (CONH). Anal. (C₂₂H₂₅FN₄O₂) calcd for C, H, N.

4.1.9 General procedure for the synthesis of the compounds 17–19.

3-(trifluoromethyl)phenyl isocyanate (1.12 g, 0.83 mL, 6 mmol) was added dropwise to a solution of the proper ethyl 2-phenyl-2,3-dihydro-1H-imidazo[1,2-*b*]pyrazole (**34**, **36**, **39**) (5mmol) in anhydrous DMF (5 mL) and the reaction mixture was refluxed for 18 h. After cooling to room temperature, the mixture was poured into an ice-water bath (50 mL) and 1M HCl solution was added until pH 5. The solid precipitated was filtered, dried on air and the purity was verified by

TLC. The crude was purified by chromatography on Silica gel using diethyl ether as eluent or recrystallized from absolute ethanol.

4.1.9.1 Ethyl 2-phenyl-1-((3-(trifluoromethyl)phenyl)carbamoyl)-2,3-dihydro-1H-imidazo[1,2-b]pyrazole-7-carboxylate 17. White solid. Yield: 36%; mp: 153–154 °C. ¹H-NMR (CDCl₃): δ 1.42 (t, *J* = 5.4, 3H, CH₃), 4.20 (near t, 1H, H3), 4.42 (q, *J* = 5.4, 2H, CH₂), 4.81 (near t, 1H, H2), 6.50 (near t, 1H, H3), 7.20–7.80 (m, 9H, Ar), 7.91 (s, 1H, H6), 11.60 (s, 1H, NH, disappears with D₂O). IR (CHCl₃): cm⁻¹ 3214 (NH), 1710–1690 (COOEt + CONH). Anal. (C₂₂H₁₉F₃N₄O₃) calcd for C, H, N.

4.1.9.2 2-Phenyl-N¹-(3-(trifluoromethyl)phenyl)-2,3-dihydro-1H-imidazo[1,2-b]pyrazole-1,7-dicarboxamide 18. White solid. Yield: 28%; mp: 226–227 °C. ¹H-NMR (DMSO-d₆): δ 3.72 (near t, 1H, H3), 4.58 (near t, 1H, H2), 5.40 (near t, 1H, H3), 7.05–7.42 (m, 10H, 9Ar + NH, 1H disappears with D₂O), 7.62 (s, 1H, H6). IR (KBr): cm⁻¹ 3450, 3223, 2871 (NH₂ + NH), 1666 (CONH₂), 1609 (CONH). Anal. (C₂₀H₁₆F₃N₅O₂) calcd for C, H, N.

4.1.9.3 2-Phenyl-7-(piperidine-1-carbonyl)-N-(3-(trifluoromethyl)phenyl)-2,3-dihydro-1H-imidazo[1,2-b]pyrazole-1-carboxamide 19. White solid. Yield: 50%; mp: 159–160 °C. ¹H-NMR (CDCl₃): δ 1.45–1.80 (m, 6H, 3CH₂-pip), 3.71–3.93 (m, 4H, 2CH₂N-pip), 4.18 (near t, 1H, H3), 4.78 (near t, 1H, H2), 6.35 (near t, 1H, H3), 7.20–7.55 (m, 9H, Ar), 7.90 (s, 1H, H6), 10.90 (s, 1H, NH, disappears with D₂O). IR (CHCl₃): cm⁻¹ 3020 (NH), 1692 (CONH), 1576 (CON-pip). Anal. (C₂₅H₂₄F₃N₅O₂) calcd for C, H, N.

4.1.10 Synthesis of ethyl 2-phenyl-2,3-dihydro-1H-imidazo[1,2-b]pyrazole-6-carboxylate 40.

Ethyl 5-amino-1-(2-hydroxy-2-phenylethyl)-1H-pyrazole-3-carboxylate (**32**) (0.27 g, 1 mmol) was dissolved in concentrated sulfuric acid (2 mL) at 0 °C and the mixture was stored at room temperature for 15 min. Then, ice-water (50 mL) was added and the solution was made neutral with NH₄OH solution. The yellow solid obtained was filtered, washed with water and recrystallized from 95% ethanol. White solid. Yield: 80%; mp 128–129 °C. ¹H-NMR (CDCl₃): δ 1.41 (t, *J* = 7.2, 3H, CH₃), 4.03 (near t, 1H, H3), 4.40 (q, *J* = 7.2, 2H, CH₂O), 4.61 (near t, 1H, H2), 4.79 (br s, 1H, NH, disappears with D₂O), 5.38 (near t, 1H, H3), 5.98 (s, 1H, H7), 7.27–7.52 (m, 5H, Ar). IR (KBr): cm⁻¹ 3350–3050 (NH), 1720 (CO). Anal. (C₁₄H₁₅N₃O₂) calcd for C, H, N.

4.1.11 General procedure for the synthesis of ethyl 1-carbamoyl-2-phenyl-2,3-dihydro-1H-imidazo[1,2-b]pyrazole-6-carboxylates 20–23.

A mixture of ethyl 2-phenyl-2,3-dihydro-1H-imidazo[1,2-b]pyrazole-6-carboxylate **40** (2.57 g, 10 mmol) and the suitable phenyl isocyanate (11 mmol) in an. DMF (30 mL) was refluxed for 18 h. After cooling to room temperature the mixture was poured into ice-water (100 mL) and 1M HCl solution was added until pH 5. The precipitated solid was filtered and dissolved in DCM (30 mL).

The solution was washed with 3 M HCl (2 x 20 mL), with water (10 mL), dried (MgSO₄) and evaporated under reduced pressure to give a crude that crystallized by adding diethyl ether.

4.1.11.1 ethyl 1-((2-fluorophenyl)carbamoyl)-2-phenyl-2,3-dihydro-1H-imidazo[1,2-b]pyrazole-6-carboxylate 20. White solid. Yield: 64%; mp 192–195 °C. ¹H-NMR (CDCl₃): δ 1.41 (t, *J* = 7.2, 3H, CH₃), 4.31 (near t, 1H, H₃), 4.40 (q, *J* = 7.2, 2H, CH₂O), 4.91 (near t, 1H, H₂), 5.88 (near t, 1H, H₃), 6.60 (s, 1H, H₇), 6.63–8.20 (m, 10H, 9Ar + NH, 1H disappears with D₂O). IR (CHCl₃): cm⁻¹ 3395 (NH), 1720–1690 (COOEt + CONH). Anal. (C₂₁H₁₉FN₄O₃) calcd for C, H, N.

4.1.11 Synthesis of 6-tert-butyl-2-phenyl-2,3-dihydro-1H-imidazo[1,2-b]pyrazole 41.

2-(5-amino-3-*tert*-butyl-1H-pyrazol-1-yl)-1-phenylethanol **33** (0.26 g, 1 mmol) was dissolved in concentrated sulfuric acid (2 mL) at 0 °C and the mixture was stored at room temperature for 15 min. Then, ice-water (50 mL) was added and the solution was made neutral with NH₄OH solution; the yellow solid obtained was filtered, washed with water and recrystallized from 95% ethanol.

Yellow solid. Yield: 78%; mp 110–112 °C. ¹H-NMR (CDCl₃): δ 1.31 (s, 9H, 3CH₃), 3.95 (near t, 1H, H₃), 4.25 (br s, 1H, NH, disappears with D₂O), 4.52 (near t, 1H, H₂), 5.22–5.40 (m, 2H, H₃ + H₇), 7.22–7.48 (m, 5H, Ar). IR (CHCl₃): cm⁻¹ 3393 (NH). Anal. (C₁₅H₁₉N₃) calcd for C, H, N.

4.1.12 General procedure for the synthesis of 6-(tert-butyl)-N,2-diphenyl-2,3-dihydro-1H-imidazo[1,2-b]pyrazole-1-carboxamides 24–27.

A mixture of 6-*tert*-butyl-2-phenyl-2,3-dihydro-1H-imidazo[1,2-b]pyrazole **41** (2.41 g, 10 mmol) and the suitable phenylisocyanate (11 mmol) in an. DMF (30 mL) was refluxed for 12 h. After cooling to room temperature, the mixture was poured into ice-water (100 mL) and 1 M HCl solution was added until pH 5. The precipitated solid was filtered and recrystallized from diethyl ether/petroleum ether (b.p. 50–60 °C) (1:1) or purified by chromatography on Silica gel, using diethyl ether as eluent.

4.1.12.1 6-(tert-butyl)-N-(2-fluorophenyl)-2-phenyl-2,3-dihydro-1H-imidazo[1,2-b]pyrazole-1-carboxamide 24. White solid. Yield: 64%; mp: 140–143 °C. ¹H-NMR (CDCl₃): δ 1.39 (s, 9H, 3CH₃), 4.23 (near t, 1H, H₃), 4.83 (near t, 1H, H₂), 5.84 (near t, 1H, H₃), 5.99 (s, 1H, H₇), 6.92–7.53 (m, 9H, Ar), 8.18 (br s, 1H, NH disappears with D₂O). IR (CHCl₃): cm⁻¹ 3020 (NH), 1695 (CONH). Anal. (C₂₂H₂₃FN₄O) calcd for C, H, N.

Analytical data for compounds **2–4**, **6–8**, **10–12**, **14–16**, **21–23**, **25–27** are available as Supporting Information.

4.2 Biology

4.2.1 Western blotting

HUVEC were seeded in a 6 well plate pre-coated with 0.2% of gelatin and Collagen G at 0.1mg/mL in PBS. The cells were cultured in M199 (GIBCO) supplemented with 10% fetal calf serum, 1% Endothelial Cell Growth Supplement (EmdMillipore), 0.1mg/mL of heparin sodium, 0.1 μ M of hydrocortisone (Sigma), 1% antibiotics-glutamine mixture, 0.1% of vitamin C for 48 h to become confluent. Confluent HUVEC were starved for at least 4 h with medium alone before stimulation. After starvation, the cells were pre-incubated with the indicated compound at 20 μ M for 10 min at 37°C and then stimulated with both VEGF at 50 ng/mL and the compound at 20 μ M for 20 min. As the compounds were dissolved in dimethylsulfoxide (DMSO), incubation with DMSO was used as control to the compounds. Treated cells were washed and lysed for protein extraction. Protein concentration was determined with the MicroBCATM Protein Assay Kit (ThermoScientific). Equal amounts of proteins (30 μ g) were subjected to a gel electrophoresis and then transferred to nitrocellulose blotting membranes. Membranes were blocked with a blocking buffer made of PBS containing 5% not-fat dry milk and 0.05% of Tween 20. Membranes were incubated overnight at 4 °C with primary antibodies diluted in the blocking buffer. The following primary antibodies were used in this study: rabbit anti-phospho-p38MAPK (pp38MAPK) (Cell signaling) used at 1:1000 dilution, rabbit anti-phospho-ERK1/2 (pERK1/2) (Cell signaling) at 1:1000 dilution, rabbit anti-phospho-Akt (pAkt) (Cell signaling) at 1:1000 dilution and mouse α -tubuline antibody (Millipore) at 1:4000 dilution. Membranes were washed three times for 5 minutes with PBS-Tween 20 0.05% and incubated at room temperature for 1 h with the adequate secondary antibody. Horseradish peroxidase (HRP)-coupled goat anti-rabbit antibody was used at dilution of 1:10000 and the HRP-Goat anti-mouse antibody at 1:3000 dilution. Both secondary antibodies were from Jackson ImmunoResearch. Membranes were washed and the signals detected using the enhanced chemiluminescence system (Advansta, WesternBrightTM Sirius). Protein band intensities were quantified with ImageJ and the tubuline intensity was used to ensure equal loaded protein amounts. The results were expressed relative to condition of treatment with VEGF and DMSO serving as control in the same blot and set at 100%. Data are representative of at least two independent experiments.

4.2.2 Wound healing assay

HUVEC were seeded in a 96-well plate for 48 h to become confluent. Once confluent cells were stained with a green tracker, the 5-chloromethylfluorescein diacetate (CMFDA) at 1:5000 (stock solution 10 mM) and the cell monolayers were injured with a sterile tip to create a scratch. Each well was washed with PBS to remove detached cells and incubated with both VEGF at 50 ng/mL

and the indicated compound at 20 μ M. The wounds were imaged just after VEGF addition and 15 h later with the ImageXpress microscope. The wound area were analysed with ImageJ to measure the colonized area in μ m [colonized area = (area T 0 h – area T 15 h)], which was then represented as a percentage of migrated cells respect to the control set at 100%. Data are representative of at least three independent experiments done in triplicate.

5. References

- [1] G.H. Algire, H.W. Chalkley, Vascular reactions of normal and malignant tissues in vivo. I. Vascular reactions of mice to wounds and to normal and neoplastic transplants, *J. Natl. Cancer Inst.* 6 (1945) 73–85.
- [2] H. Allgayer, R. Babic, K.U. Gruetzner, A. Tarabichi, F.W. Schildberg, M.M. Heiss, c-ErbB-2 is of independent prognostic relevance in gastric cancer and is associated with the expression of tumor-associated protease systems, *J. Clin. Oncol.* 18 (2000) 2201–2209.
- [3] S.B. Bressler, Introduction: understanding the role of angiogenesis and antiangiogenic agents in age-related macular degeneration, *Ophthalmology* 116 (2009) S1–S7.
- [4] T.P. Padera, B.R. Stoll, J.B. Tooredman, D. Capen, E. di Tomaso, R.K.Jain, Pathology: cancer cells compress intratumour vessels, *Nature* 427 (2004) 695.
- [5] M. Paez-Ribes, E. Allen, J. Hudock, T. Takeda, H. Okuyama, F. Vinals, M. Inoue, G. Bergers, D. Hanahan, O. Casanovas, Antiangiogenic therapy elicits malignant progression of tumors to increased local invasion and distant metastasis, *Cancer Cell* 15 (2009) 220–231.
- [6] J.P. Thiery, H. Acloque, R.Y. Huang, M.A. Nieto, Epithelial–mesenchymal transitions in development and disease, *Cell* 139 (2009) 871–890.
- [7] I. del Barco Barrantes, A.R. Nebreda, Roles of p38MAPKs in invasion and metastasis, *Biochem. Soc. Trans.* (2012) 40, 79-84.
- [8] O. Bruno, C. Brullo, F. Bondavalli, S. Schenone, A. Ranise, N. Arduino, M. B. Bertolotto, F. Montecucco, L. Ottonello, F. Dallegri, M. Tognolini, V. Ballabeni, S. Bertoni, E. Barocelli, Synthesis and biological evaluation of N-pyrazolyl-N'-alkyl/benzyl/phenylureas: a new class of potent inhibitors of interleukin 8-induced neutrophil chemotaxis, *J. Med. Chem.* 50 (2007) 3618-3626.
- [9] O. Bruno, C. Brullo, F. Bondavalli, S. Schenone, S. Spisani, M.S. Falzarano, K. Varani, E. Barocelli, V. Ballabeni, C. Giorgio, M. Tognolini, 1-Methyl and 1-(2-hydroxyalkyl)-5-(3-

alkyl/cycloalkyl/phenyl/naphthylureido)-1H-pyrazole-4-carboxylic acid ethyl esters as potent human neutrophil chemotaxis inhibitors, *Bioorg. Med. Chem.* 17 (2009) 3379-3387.

[10] M. Bertolotto, C. Brullo, L. Ottonello, F. Montecucco, F. Dallegri, O. Bruno, Treatment with 1-(2-hydroxyalkyl)-5-(3-alkyl/phenyl/naphthylureido)-1H-pyrazole-4-carboxylic acid ethyl esters abrogates neutrophil migration towards fMLP and CXCL8 via the inhibition of defined signalling pathways, *Eur J Clin Invest*, 2014, 44.

[11] O. Bruno, C. Brullo, F. Bondavalli, A. Ranise, S. Schenone, M. S. Falzarano, K. Varani, S. Spisani, Phenyl-2,3-dihydro-1H-imidazo[1,2-b]pyrazole derivatives: new potent inhibitors of fMLP-induced neutrophil chemotaxis, *Bioorg. Med. Chem. Lett.* 17 (2007) 3696-3701.

[12] C. Brullo, S. Spisani, R. Selvatici, O. Bruno, N-Aryl-2-phenyl-2,3-dihydro-imidazo[1,2-b]pyrazole-1-carboxamides 7-substituted strongly inhibiting both fMLP-OMe- and IL-8-induced human neutrophil chemotaxis, *Eur. J. Med. Chem.* 47 (2012) 573-579.

[13] R. Selvatici, C. Brullo, O. Bruno, S. Spisani, Differential inhibition of signaling pathways by two new imidazo-pyrazoles molecules in fMLF-OMe- and IL8-stimulated human neutrophil, *Eur. J. Pharmacol.* 718 (2013) 428-434.

[14] C. Xi, F. Junfa, F. Pingchen, A. Krasinski, L. Li, R.M. Lui, McMahan, P. Jeffrey, J.P. Powers, Z. Yibin, P. Zhang, Preparation of aza-aryl 1H-pyrazol-1-yl benzenesulfonamides as CCR9 antagonists U.S. Pat. Appl. Publ. (2013), US 20130225580 A1.

Design, synthesis and biological evaluation of new pyrazolyl-ureas and imidazopyrazol-carboxamides able to interfere with p38MAPK and other kinases involved in tumor cell migration

Elda Meta, Chiara Brullo, Adama Sidibe, Beat A. Imhof, Olga Bruno

Highlights

- New of pyrazolylureas and imidazopyrazolylcarboxamides are reported.
- Activity on the phosphorylation of ERK1/2, p38MAPK and Akt in HUVEC cells was investigated.
- SAR consideration revealed a different trend in increasing or inhibiting p38MAPK, ERK1/2 and Akt phosphorylation.
- Specific substituents in pyrazole nucleus differently interfere with VEGF-induced signaling.
- Carboxyethyl substituent on the pyrazole serve like a switch between increasing or decreasing the kinase phosphorylation levels.
- New compounds might interfere on angiogenesis and with different upstream target kinases on the MAPK and PI3K pathways.
- Compound 3 showed a significant inhibitory effect on endothelial cell migration, a key function for angiogenesis.